AGU PUBLICATIONS

JGR

Journal of Geophysical Research: Atmospheres

RESEARCH ARTICLE
10.1002/2015JD024045

Key Points:
- The Great Plains low-level jet modifies low-level vorticity over the central Gulf States
- Intensified southerly wind over the southern Great Plains weakens vorticity and suppresses precipitation
- Southerly inflow over the Gulf of Mexico increases precipitation over the central Gulf States

Correspondence to:
B. Pu,
bing.pu@noaa.gov

Citation:
Pu, B., R. E. Dickinson, and R. Fu (2016), Dynamical connection between Great Plains low-level winds and variability of central Gulf States precipitation, *J. Geophys. Res. Atmos., 121*, 3421–3434, doi:10.1002/2015JD024045.

Received 4 AUG 2015
Accepted 23 MAR 2016
Accepted article online 30 MAR 2016
Published online 14 APR 2016

Dynamical connection between Great Plains low-level winds and variability of central Gulf States precipitation

Bing Pu[1,2], Robert E. Dickinson[1], and Rong Fu[1]

[1]Department of Geological Sciences, Jackson School of Geosciences, University of Texas at Austin, Austin, Texas, USA, [2]Now at Atmospheric and Oceanic Sciences, Princeton University, NOAA/Geophysical Fluid Dynamics Laboratory, Princeton, New Jersey, USA

Abstract The Great Plains low-level jet has been related to summer precipitation over the northern Great Plains and Midwest through its moisture transport and convergence at the jet exit area. Much less studied has been its negative relationship with precipitation over the southern Great Plains and the Gulf coastal area. This work shows that the southerly low-level winds at 30°–40°N over the southern Great Plains are significantly correlated with anticyclonic vorticity to its east over the central Gulf States (30°–35°N, 85°–95°W) from May to July. When the low-level jet is strong in June and July, anomalous anticyclonic vorticity over the central Gulf States leads to divergence and consequent subsidence suppressing precipitation over that region. In contrast, an enhanced southerly flow at the entrance region of the jet over the Gulf of Mexico, largely uncorrelated with the meridional wind over the southern Great Plains, is correlated with increased precipitation over the central Gulf States. Precipitation is large over the central Gulf States when the meridional wind over the southern Great Plains is weakest and over the Gulf of Mexico is strongest. This increase is consistent with the increased moisture transport and dynamic balance between loss of vorticity by advection and friction and gain by convergence.

1. Introduction

Much of the precipitation in the Southeast, South-central, and Midwest U.S. is supplied by moisture flux originating in the Western Atlantic and Gulf of Mexico on the equatorwardside of the North Atlantic subtropical high [e.g., *Rasmusson*, 1967], and the latter includes on its western side, the Great Plains low-level jet (LLJ) [e.g., *Helfand and Schubert*, 1995; *Weaver and Nigam*, 2008]. The LLJ extends from about 20°N over the Gulf of Mexico to the northern Great Plains and Midwest, with its core located around 95°–102°W over the southern Great Plains (Figure 1) at 850–950 hPa.

The LLJ affects the variability of warm season precipitation over the central U.S. and Midwest on multiple time scales [e.g., *Hering and Borden*, 1962; *Pitchford and London*, 1962; *Higgins et al.*, 1997; *Schubert et al.*, 1998; *Weaver and Nigam*, 2008]. Severe floods or droughts over the Great Plains have been related to abnormal moisture transport by the LLJ or lack of it [e.g., *Mo et al.*, 1997; *Weaver et al.*, 2009]. Besides supplying moisture, the Great Plains LLJ affects summer precipitation by setting up meridional convergence of the meridional wind (i.e., $-\partial v/\partial y$, v represents north-south component of wind) at its exit area over the northern Great Plains and Midwest [e.g., *Arritt and Mitchell*, 1994; *Weaver and Nigam*, 2008; *Weaver et al.*, 2009; *Weaver and Nigam*, 2011].

By comparison, reasons for a negative relationship between the LLJ and precipitation over the Gulf coast [e.g., *Weaver and Nigam*, 2008] (also Figure 1), especially to the east of the jet core over the central Gulf States (CGS box in Figure 1), have not been clear. *Weaver and Nigam* [2008] first examined the empirical orthogonal function (EOF) pattern of 900 hPa v wind in the jet region in July and found that the positive phases of the second and third EOF modes, representing a meridional shift of the jet core and an "in-place strengthening" of the jet, respectively, were negatively correlated with precipitation over the Gulf States (their Figures 10 and 12; pages 1546 and 1549). They suggested that the meridional wind gradient (i.e., $\partial v/\partial y$) alone could not explain such negative correlations. This paper hypothesizes that vorticity to the east of the jet core, mainly from the zonal gradient of the meridional wind (i.e., $\partial v/\partial x$), is a primary control on the convergence and thus also precipitation over the central Gulf States.

Pu and Dickinson [2014] have previously related diurnal variations of the Great Plains LLJ to vorticity anomalies to the east of the jet core resulting from variations of the zonal gradient of meridional wind over the eastern plains.

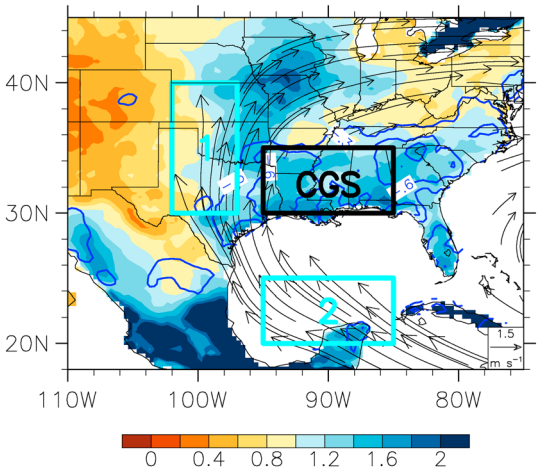

Figure 1. Standard deviation (mm d^{-1}) of June and July precipitation in the NARR from 1979 to 2013. Vectors are climatological 900 hPa winds with wind magnitude ≥ 3 m s^{-1}. The black box denotes the averaging area for central Gulf States precipitation (30°–35°N and 85°–95°W). Blue contours show July precipitation regressed onto the Great Plains LLJ index defined by *Weaver and Nigam* [2008] and only negative anomalies equal to or lower than -0.3 mm d^{-1} (contour intervals: 0.3 mm d^{-1}) are plotted to highlight its connection with Gulf States precipitation. Boxes "1" and "2" denote the averaging area of the V_SGP and V_GF indices (section 3.1), respectively.

Convergence and rising motion develop from an anomalous positive vorticity tendency and thus promote convective precipitation. In this work, we show, on interannual time scales, how changes of meridional winds over the southern Great Plains and the Gulf of Mexico that lead to modification of vorticity and its advection over the central Gulf States are associated with anomalous moisture divergence and precipitation variations.

The interannual variability of precipitation over the eastern Gulf States to southeastern U.S. has been related to tropical Atlantic sea surface temperatures (SSTs) [e.g., *Wang et al.*, 2010], natural atmospheric variability [e.g., *Seager et al.*, 2009], the location of the North Atlantic Subtropical high [*Li et al.*, 2011, 2012] in summer, and to tropical Pacific SSTs in winter [e.g, *Mo and Schemm*, 2008]. Some of the same dynamical processes, e.g., the variations of the North Atlantic Subtropical high, may affect all these regions (i.e., Gulf States and the southeastern U.S.) by modifying the magnitude of the Great Plains LLJ [e.g., *Zhu and Liang*, 2013]. Here we mainly focus on understanding the direct connections between the low-level winds and precipitation over the central Gulf States and do not examine other factors determining these winds or otherwise contributing to the variability of the precipitation.

In sections 2 and 3, we introduce the reanalysis product and methodology used in this study. In section 4, we present our analysis of the relationship between low-level meridional winds over the southern Great Plains and the Gulf of Mexico, vorticity, and central Gulf States precipitation on different time scales. Major conclusions are summarized in section 5.

2. Reanalysis

The North American Regional Reanalysis (NARR) [*Mesinger et al.*, 2006] provides high spatial (~32 km horizontally and 29 vertical levels from 1000 hPa to 100 hPa with intervals of 25 hPa between 1000 hPa and 700 hPa) and temporal (3-hourly) resolution data over the U.S. from 1979 to present. Its high spatial resolution is quite suitable for studying the variability of the LLJ and vorticity over the central Gulf States, which cover 5° of latitude and 10° of longitude. Differing from other reanalysis products, precipitation in the NARR is assimilated from observations and has been used to study the variability of the Great Plains LLJ and precipitation on diurnal to interannual time scales [e.g., *Ruiz-Barradas and Nigam*, 2006; *Ruane*, 2010; *Pu and Dickinson*, 2014]. Here 3-hourly, daily, and monthly variables of horizontal winds, geopotential heights, specific humidity, and precipitation from 1979 to 2013 are used to analyze the connection between the jet and precipitation during May, June, and July, with a focus on June and July, when the jet reaches its maximum speed in its core area.

3. Methodology

3.1. Precipitation and Wind Indices

To efficiently characterize the relationship between precipitation and the low-level meridional wind over the southern Great Plains and central Gulf States, we define a suite of indices as listed in Table 1. A central Gulf States precipitation index is defined as the average of precipitation over the spatial domain of 30°–35°N and 85°–95°W (P_CGS; Figure 1). The area is chosen based on its relatively high standard deviation of June and July precipitation and as the center of the region in which precipitation is negatively related to the Great Plains LLJ (Figure 1).

Table 1. List of the Indices Used in the Paper

Indices	Definition	Usage
V_SGP index	Averaged 900 hPa meridional wind speed between 30°–40°N and 97°–102°W	Represents the LLJ over the southern Great Plains and the southerly inflow over the Gulf of Mexico
V_GF index	Averaged 900 hPa meridional wind speed between 20°–25°N and 85°–95°W	
CGS precipitation (P_CGS), vorticity, and moisture divergence/convergence indices	Averaged precipitation, 900 hPa vorticity and moisture divergence/convergence over the central Gulf States (CGS; 30°–35°N, 85°–95°W) on monthly mean (section 4.1) and on 3-hourly scales (section 4.2)	To examine the connection between the LLJ and precipitation over the central Gulf States
V_SGP-GF index	V_SGP index minus V_GF index	A wind index combines both meridional flows and is highly correlated with the P_CGS index
Reconstructed CGS precipitation index (regP)	Calculated using V_SGP and V_GF indices and their regression coefficients with the P_CGS index	To examine to what extent that the precipitation over the central Gulf States can be represented by the meridional wind indices

Because this work aims to clarify the potential influence of the LLJ over the southern Great Plains and Gulf of Mexico on vorticity, moisture convergence, and consequently precipitation over the central Gulf States, we define two meridional wind indices, representing the LLJ over the southern Great Plains and its Gulf inflow, and referred to as V_SGP and V_GF, respectively.

The V_SGP index is calculated by averaging 900 hPa meridional winds over the southern Great Plains between 97°–102°W and 30°–40°N (Box 1 in Figure 1). *Weaver and Nigam* [2008] found that the jet core was located between 97°–102°W and 25°N–35°N at 900 hPa in the NARR. Our index uses the same range in longitude but shifts the averaging area 5° northward to better capture the relationship between vorticity and precipitation variations over the central Gulf States (see discussion in section 4). The V_GF index is defined by averaging 900 hPa meridional winds between 20°–25°N and 85°–95°W (Box 2 in Figure 1). The domain captures the geographical location of the southerly inflow in the jet entrance region over the Gulf of Mexico. We tested the sensitivity of the results to the averaging areas of the V_GF and V_SGP indices by slightly shifting the domains to 90°–95°W and 20°–25°N for the V_GF index, and 97°–102°W and 25°–35°N for the V_SGP index, respectively; the correlations and regression values changed slightly, but the conclusions remained the same.

3.2. Composite Analysis

To examine the connection between the low-level meridional wind over the southern Great Plains and Gulf of Mexico and the precipitation over the central Gulf States, we calculated composites of the precipitation, relative vorticity at 900 hPa, and terms determining vorticity balance for the seven strongest and seven weakest years of the June and July V_SGP and V_GF indices (Table 2), respectively, representing about 20% of the 35 years of our analysis period. Their differences, i.e., derived from strong minus weak years, provide the anomaly patterns discussed in section 4.

3.3. Vorticity Budget

A vorticity budget is calculated to diagnose the major sources and sinks of anomalous vorticity in the strong and weak meridional-wind-index composites and the relationship between low-level vorticity and convergence. Over the central Gulf States precipitation is primarily maintained by moisture convergence (dominated by convergence), i.e., local evaporation contributes only about 15–16% to the total

Table 2. List of Years Used in the Composites of Strong and Weak Southerly Flows Over the Southern Great Plains and Over the Gulf of Mexico Based on the Meridional Wind Indices (V_SGP and V_GF) During June and July

		Years
V_SGP	Strong	2011, 1993, 2008, 2002, 2010, 2005, 2012
	Weak	1989, 1985, 2009, 1988, 1996, 1992, 1995
V_GF	Strong	1989, 1998, 2003, 1994, 1993, 1981, 2001
	Weak	2006, 1988, 1995, 2005, 2012, 2011, 2013

precipitation in June and July based on the NARR. The vorticity equation derived from the primitive horizontal momentum equations is as follows:

$$\frac{\partial \zeta}{\partial t} = -\vec{V}\cdot\nabla(\zeta+f) - (\zeta+f)\nabla\cdot\vec{V} + k\cdot\left(\frac{\partial \vec{V}}{\partial p}\times\nabla\omega\right) - \omega\frac{\partial\zeta}{\partial p} + k\cdot\left(\nabla\times\vec{F}\right), \quad (1)$$

where ζ is relative vorticity, $\vec{V}=(u,v)$ is horizontal wind vector, ω is vertical p velocity, $f\cong 2\Omega\sin\phi$ is the Coriolis parameter, $\Omega = 7.292\times10^{-5}\,s^{-1}$ is the angular velocity of rotation of the earth, ϕ is latitude, $\vec{F}=(F_x,F_y)$ is friction (i.e., the turbulent vertical momentum fluxes from the boundary layer to surface), and k is the unit vector in the vertical direction. $\partial\zeta/\partial t$ on the left-hand side of equation (1) is the vorticity tendency. The five terms on the right-hand side represent changes of the vorticity tendency due to horizontal advection, convergence, tilting, vertical transport of vorticity, and near-surface friction, respectively.

In the composite analysis, each variable of equation (1) can be written in terms of composite mean, monthly departure from the composite mean, and daily departure from the monthly mean. For instance, $u=\overline{\overline{u}}+\overline{u}'+u'$, where u is daily zonal wind, $\overline{\overline{u}}$ is the composite mean of monthly mean zonal wind, $\bar{u}'$ is monthly departure from the composite mean, and u' is daily departure from the monthly mean. Taking the time mean average over the years within a composite, we write equation (1) as follows

$$\frac{\partial\overline{\overline{\zeta}}}{\partial t} = -\overline{\overline{\vec{V}}}\cdot\nabla\left(\overline{\overline{\zeta}}+f\right) - \left(\overline{\overline{\zeta}}+f\right)\nabla\cdot\overline{\overline{\vec{V}}} + k\cdot\left(\frac{\partial\overline{\overline{\vec{V}}}}{\partial p}\times\nabla\overline{\overline{\omega}}\right) - \overline{\overline{\omega}}\frac{\partial\overline{\overline{\zeta}}}{\partial p} + k\cdot\left(\nabla\times\overline{\overline{\vec{F}}}\right) + \text{trans}\approx 0 \quad , \quad (2)$$

where a double overbar $(\bar{\bar{\ }})$ denotes composite mean. The last term on the right-hand side of equation (2) is the vorticity tendency contributed by transient eddies. It contains two parts representing contributions from daily and monthly departures, i.e., $\text{trans} = \overline{\text{trans}_{\text{daily}}} + \overline{\text{trans}_{\text{monthly}}}$, where

$$\text{trans}_{\text{daily}} = \overline{\vec{V}'\cdot\nabla\zeta'} - \overline{\zeta'\nabla\cdot\vec{V}'} + \overline{k\cdot\left(\frac{\partial\vec{V}'}{\partial p}\times\nabla\omega'\right)} - \overline{\omega'\frac{\partial\zeta'}{\partial p}} \quad , \quad (3)$$

and

$$\text{trans}_{\text{monthly}} = \overline{\vec{V}'}\cdot\nabla\overline{\zeta}' - \overline{\zeta}'\nabla\cdot\overline{\vec{V}'} + k\cdot\left(\frac{\partial\overline{\vec{V}'}}{\partial p}\times\nabla\overline{\omega'}\right) - \overline{\omega'}\frac{\partial\overline{\zeta'}}{\partial p} \quad . \quad (4)$$

The overbar $(\bar{\ })$ denotes averaging over a month, overbar prime $(\bar{\ }')$ denotes monthly departure, and prime $(')$ denotes daily departures. For calculation of equation (2), we use the 900 hPa daily and monthly horizontal winds of the NARR data, regarding them as an approximation to a vertical average over the boundary layer. The vertical gradients at 900 hPa $(\partial/\partial p)$ are computed using horizontal wind and vorticity at 925 hPa and 875 hPa, respectively. All the dynamical transients terms equations (3) and (4) were found to be one order of magnitude or more smaller. The friction term in equation (2) is calculated as a residual after explicitly calculating all the other terms in the equation. The vorticity tendency is approximately zero for a long-time average as adjustment between vorticity, its tendency, and convergence is very fast, i.e., within a day in a simplified boundary layer model [e.g., *Pu and Dickinson*, 2014]. Our calculation here also confirmed that the $\partial\overline{\overline{\zeta}}/\partial t$ term is about two orders of magnitude smaller than the other terms and can be neglected. The tilting and vertical transport of vorticity terms were each found to be very small, and therefore, equation (2) is approximated by a balance among the three largest terms on the right-hand side, i.e., the advection term, convergence term, and friction (residual) term.

3.4. Bootstrap Test

To examine the statistical significance of the differences between the strong and weak composites of the V_SGP and V_GF indices, bootstrapping resampling is applied. First, two 7 year composites, each by randomly sampling individual years from the whole period (1979–2013), are formed, and then the differences between the two composites are calculated. This process is repeated for 10,000 times to obtain the 2.5% and 97.5% levels for the differences. The differences between the strong and weak wind composites are considered

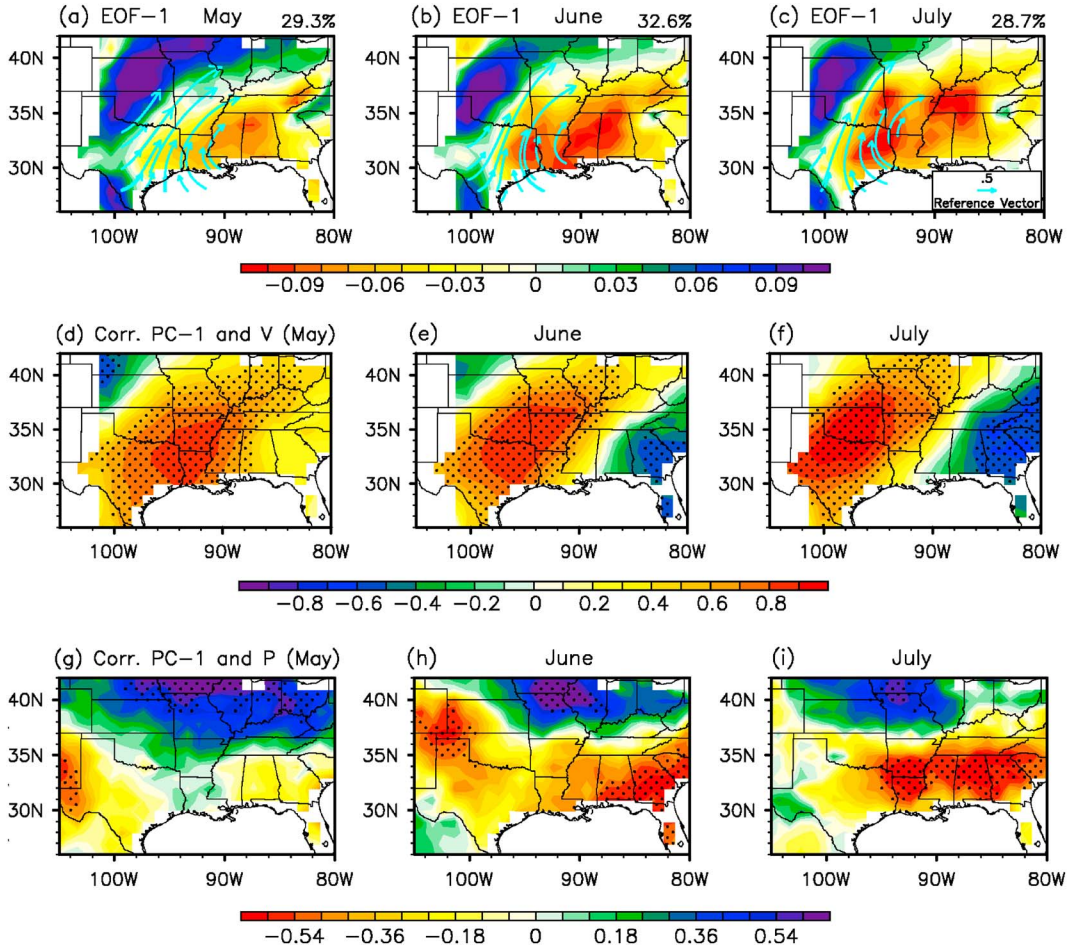

Figure 2. (a–c) EOF-1 of 900 hPa relative vorticity over land for May, June, and July and (d–f) the correlations between EOF-1 time series (PC-1) and 900 hPa meridional wind and (g–i) correlations between PC-1 and precipitation from 1979 to 2013. Vectors in Figures 2a–2c are rotational winds calculated from the pattern of vorticity EOFs (section 3.5). Areas with correlation coefficients significant at the 99% confidence level (*t* test) are dotted. Elevations higher than that of 900 hPa on the eastern edge of the Rockies are masked out.

significant at the 95% confidence level when they equal or exceed the 97.5% level or are equal or less than the 2.5% level.

3.5. EOF Analysis

Here EOF analysis [e.g., *North et al.*, 1982] is applied to the 900 hPa monthly relative vorticity ($\zeta = \frac{\partial v}{\partial x} - \frac{\partial u}{\partial y}$) field, which is calculated from 900 hPa monthly horizontal winds in the NARR, for May, June, and July, respectively, from 1979–2013, to show the development of summer vorticity field. To reveal the connection between the vorticity spatial patterns and the LLJ, we first calculated wind patterns directly associated with the vorticity EOFs, i.e., the rotational winds ($u = \partial\psi/\partial y$, $v = -\partial\psi/\partial x$), where the stream function ψ is solved from the vorticity EOFs ($\nabla^2\psi = -\zeta$). The time series of EOF-1 is then correlated with the full component of meridional wind and precipitation field to reveal their connections.

4. Results

4.1. Connection Between the Great Plains LLJ and Central Gulf States Precipitation on an Interannual Time Scale

To examine the hypothesis that the LLJ is associated with the interannual variability of the vorticity to its east and consequently central Gulf States precipitation, we first look at the dominant patterns of low-level vorticity in the region and related winds. Figures 2a–2c show EOF-1 of 900 hPa relative vorticity (ζ) for May, June,

Table 3. Correlations Between Central Gulf States Precipitation Index (P_CGS), V_SGP, V_GF, V_SGP-GF Indices (See Text), and Reconstructed Central Gulf States Precipitation Indices (regP, Table 1) in May, June, July, and June and July (JJ) Average[a]

Correlation	JJ	May	June	July
P_CGS and V_SGP	**−0.53**	*−0.25*	**−0.47**	**−0.62**
P_CGS and V_GF	**0.53**	**0.61**	**0.62**	**0.47**
P_CSG and V_SGP-GF index	**−0.73**	**−0.60**	**−0.75**	**−0.76**
V_SGP and V_GF	*−0.06*	*−0.02*	*−0.04*	*−0.03*
P_CGS and regP	**0.73**	**0.66**	**0.76**	**0.77**

[a]Correlation coefficients that do not reach the 95% confidence level (*t* test) are in Italics, while the rest are significant.

and July, respectively. The 900 hPa is selected because that is the level of peak meridional wind speed of the LLJ [*Weaver and Nigam*, 2008]. The analysis of vorticity in May is included here to show the development of summer vorticity field. About 29–33% of the variance of relative vorticity is explained by EOF-1 for May, June, and July (Figures 2a–2c), while EOF-2 explains 15–21% of the variance over these months. The remaining components each explain less than 10% of the total variance. The EOF-1 in May has a negative center along the Gulf coast and positive over the northwestern Plains (Figure 2a). The magnitude of this pattern increases over the eastern Plains and central Gulf States in progressing into summer (Figures 2b and 2c). EOF-2 has a similar east-west dipole pattern of positive and negative vorticity anomalies on the western and eastern sides of Great Plains, but its negative vorticity anomaly is located further to the north at about 35°–45°N, representing the variations of vorticity over the northern Great Plains and Midwest rather than over the central Gulf States, and thus is not shown. The rotational part of the winds retrieved from the vorticity EOF-1 s (see methods in section 3.5) reveal the wind patterns directly associated with the vorticity patterns. As shown in Figures 2a–2c, the rotational winds are located over the southern Great Plains in between the negative and positive vorticity anomaly centers. Figures 2d–2f show the correlations between first principal components (i.e., time series; PC-1 s) and 900 hPa meridional winds for May, June, and July, respectively. The positive correlation centers are located over the southern Great Plains and extend toward the Midwest. From May to July, these significantly positive correlation areas become stronger and extend more northward, with an intensified zonal gradient over the Great Plains associated with the development of the anticyclonic vorticity center. The strongest such correlations occur in July when the wind in the jet area is mostly southerly [cf. *Weaver and Nigam*, 2008; their Figure 3, page 1538] and these correlations are centered slightly north of the jet core (i.e., 97°–102°W, 25°–35°N) over the southern Great Plains, consistent with the location of strongest negative vorticity anomalies (Figure 2c). Figures 2g–2i show the correlations between PC-1 s and precipitation. The dipole pattern of relative vorticity (Figures 2a–2c) is associated with increased precipitation over the northern Great Plains and Midwest, and reduced precipitation along the Gulf coast, most of Texas and the Southeast, especially in June and July.

In sum, Figure 2 shows that an east-west dipole pattern of positive and negative relative vorticity anomalies are associated with the Great Plains LLJ on the interannual time scale. In particular, an intensified jet over the southern Great Plains is accompanied by anticyclonic vorticity and decreased precipitation over the central Gulf States.

The V_SGP index, representing the magnitude of the meridional wind over the southern Great Plains, is significantly (95% confidence level) negatively correlated with precipitation over the central Gulf States (P_CGS) in June and July (Table 3) and can explain about 28% of precipitation variances in June and July. What's the contribution of the southerly Gulf inflow (represented by the V_GF index) to the precipitation over the central Gulf States? Table 3 shows that the V_GF index is significantly positively correlated with the P_CGS index from May to July, with higher correlations in May and June of around 0.61. During June and July, it also explains about 28% of the precipitation variances, i.e., the same as the V_SGP index.

Figure 3 further demonstrates the connection of the Gulf and southern Great Plains meridional winds to 900 hPa vorticity, moisture flux ($q\vec{V}$), and precipitation using a composite analysis based on the magnitude of the V_SGP and V_GF indices. Here the differences between patterns derived from the strong and weak composites of the V_SGP and V_GF indices are shown to demonstrate the patterns of vorticity and precipitation changes. Strong southerly winds over the southern Great Plains are associated with a negative vorticity anomaly over the central Gulf States and southeastern U.S. (Figure 3a), consistent with the correlations shown in Figures 2d–2f, i.e.,

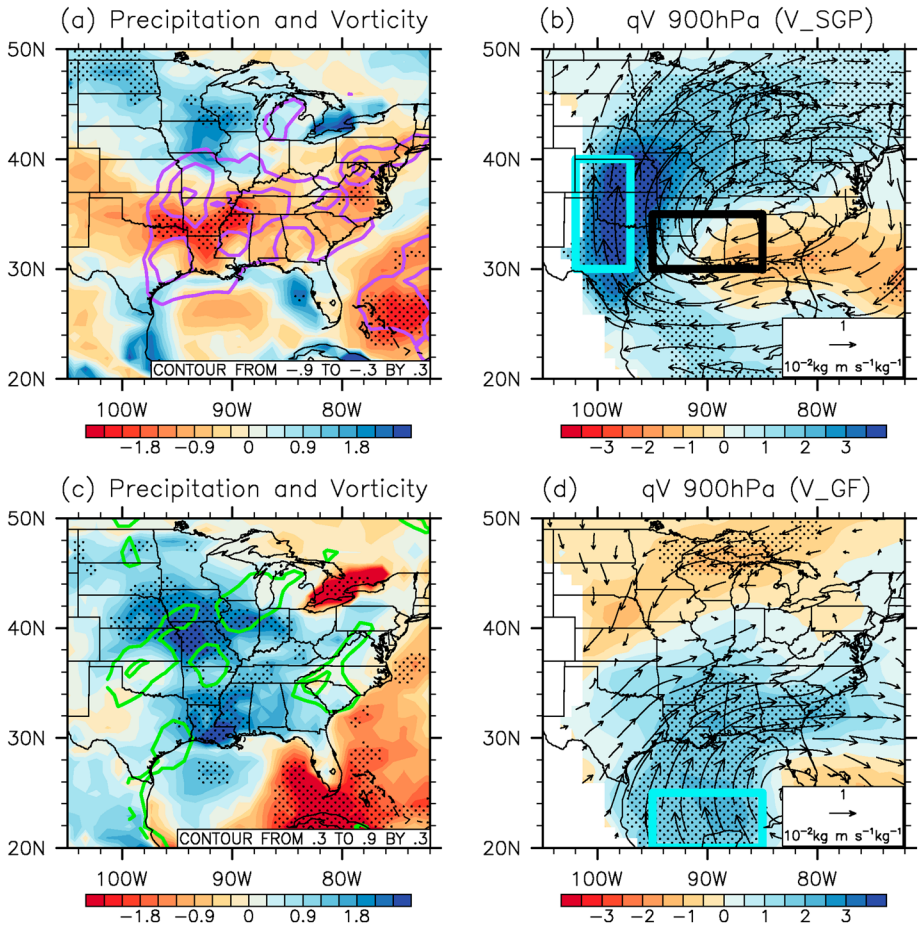

Figure 3. Differences of (a, c) precipitation (mm d^{-1}; shading) and 900 hPa vorticity (10^{-5} s^{-1}; contours), (b, d) 900 hPa moisture flux (vector; 10^{-2} kg m s^{-1} kg^{-1}) and magnitude of moisture flux (shading; 10^{-2} kg m s^{-1} kg^{-1}) (a and b) between strong and weak V_SGP composites and (c and d) between strong and weak V_GF composites (Table 2) averaged from June to July. Cyan boxes denote averaging areas for V_SGP and V_GF indices, the black box indicates the central Gulf States region. Areas significant at the 95% confidence level are dotted (bootstrap test). Only negative (purple) vorticity anomalies (0.3 10^{-5} s^{-1}intervals) in Figure 3a and positive (green) anomalies in Figure 3c are shown.

enhanced southerly winds over the southern Great Plains are positively associated with a negative relative vorticity anomaly over the central Gulf states. Moisture flux is enhanced over the southern Great Plains up to the western side of the central Gulf States box but reduced from the eastern side of the box (Figure 3b). Precipitation over the central Gulf States is suppressed by the anomalous anticyclonic vorticity determined by negative shear (i.e., largely from $\partial v/\partial x < 0$) to the east of the LLJ, despite enhanced moisture flux on its western side.

Enhanced Gulf southerly flow is associated with increased precipitation over both the central Gulf States and northern Great Plains (Figure 3c). The latter is associated with anomalous cyclonic vorticity over the northern Great Plains (i.e., largely from $-\partial u/\partial y > 0$), while vorticity anomalies over the Gulf coast are relatively small. The enhanced northward moisture transport from the Gulf of Mexico (Figure 3d) and resultant moisture convergence contribute to the precipitation increase over the central Gulf States.

Our analysis of low-level vorticity budgets provides an understanding of the link between the meridional winds and precipitation over the central Gulf States, especially, through the coupling between low-level vorticity and divergence fields. Figures 4a–4f show the three largest terms in equation (2), (i.e., the vorticity equation) from the composite analysis, i.e., the convergence, vorticity advection, and friction (friction is calculated as a residual but that could also contain some numerical errors) terms. The rest of the terms in equation (2) are very small. The values of each term averaged over the central Gulf States are labeled on the figures. Positive values in the left-side frames (first column) indicate positive vorticity tendency (i.e., a vortex stretching) associated with convergence, the middle frames (second column) southward vorticity

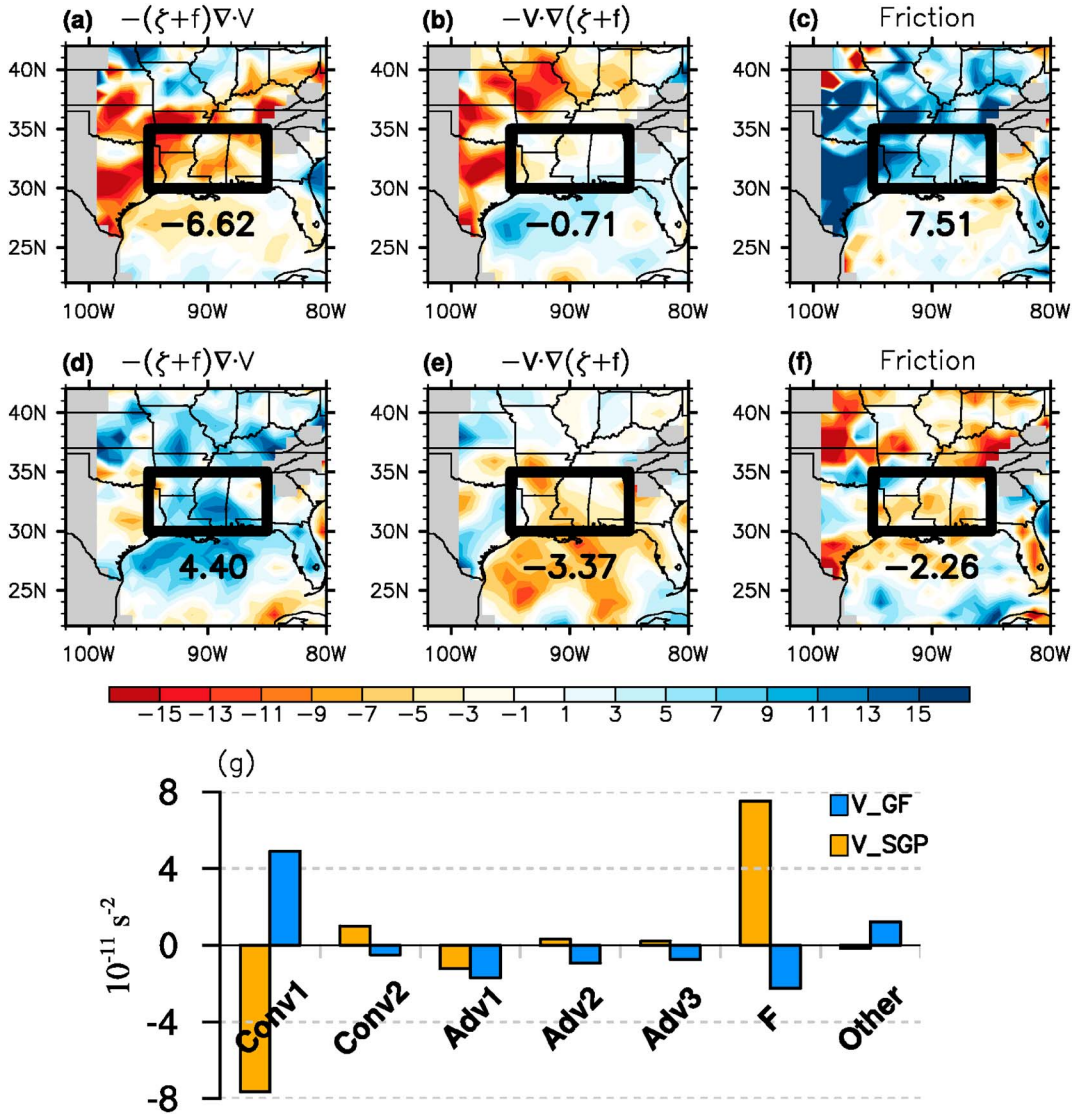

Figure 4. Differences of three vorticity equation terms, (a, d) convergence term, (b, e) advection term, and friction term (calculated as a residual), from equation (2) at 900 hPa during June and July (a–c) between strong and weak V_SGP composites and (d–f) between strong and weak V_GF composites. Values averaged over the central Gulf States (black boxes) are printed below the boxes. (g) Values of each term in equation (2) averaged over the central Gulf States box for the differences between strong and weak V_SGP composites (orange) and differences between strong and weak V_GF composites (blue). "Conv1" denotes $-f\nabla\cdot\vec{V}$, and "Conv2" denotes $-\zeta\nabla\cdot\vec{V}$, and "Adv1" denotes $-\beta\bar{v}$, "Adv2" denotes $-\bar{u}\partial\bar{\zeta}/\partial x$, "Adv3" denotes $-\bar{v}\partial\bar{\zeta}/\partial y$, "F" denotes friction, and "Other" denotes the sum of tilting term, dynamical transient term, vertical transport, and vorticity tendency terms. Units: 10^{-11} s^{-2}. Topography is masked out by grey shading.

advection, and the right frames (third column) frictional loss of anticyclonic vorticity (as estimated by the residual term), and for negative values, vice versa. The convergence terms of the left frames are largely proportional to moisture convergence hence imply a positive precipitation anomaly. The magnitudes of the individual terms in equation (2) averaged over the central Gulf States are shown in Figure 4g.

Around 32.5°N, relative vorticity (ζ) over the central Gulf States is about one order of magnitude smaller than the Coriolis parameter (f), thus away from regions of strong shear, i.e., away from the large vorticity gradients indicated in Figure 3a, $f+\zeta \approx f$. The convergence term is dominated by $-f\nabla\cdot\vec{V}$ (Conv1 in Figure 4g). The advection term is not only largely contributed by $-\beta\bar{v}$ (Adv1), where $\beta = df/dy$, over the region with strong meridional wind, e.g., over the Great Plains in Figure 4b and over the Gulf in Figure 4e but also contains contributions from both zonal and meridional advection of vorticity gradients (Adv2 and Adv3).

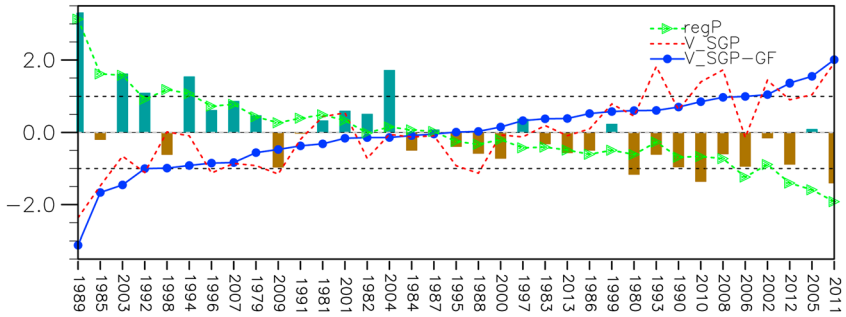

Figure 5. Time series of precipitation over the central Gulf States (dark green and brown bars; P_CGS), V_SGP-GF index (blue), V_SGP index (red dashed) from the NARR and reconstructed precipitation index using the two meridional wind indices (regP; green) averaged over June and July. All the indices are standardized and reordered according to the rank of the V_SGP-GF index.

The top frames of Figure 4 show the balance for the V_SGP composite anomalies. Over the Gulf the friction term is small (Figure 4c) and so the first two terms approximately balance (Figures 4a and 4b). Here low-level wind anomalies are not shown but their patterns closely resemble the patterns of moisture flux in Figure 3b. Over the southeastern U.S. and central Gulf States the dominant balance for the V_SGP composite anomaly patterns is between frictional loss of anticyclonic vorticity (Figure 4c) and its generation by vortex tube contraction associated with horizontal divergence (Figure 4a), as occurred in our previous study on a daily mean scale [*Pu and Dickinson*, 2014], which found that in the jet region on this scale divergence was largely balanced by the near-surface friction. Over some areas where the southerly wind speed anomaly is relatively large, e.g., northeastern Texas and Missouri, the northward vorticity advection (Figure 4b) increases anticyclonic vorticity, i.e., weakens the effect of the friction term, and balance requires all three terms.

The second row of frames shows the balance for the V_GF composite anomalies. Figure 4d shows convergence centered around 32° N and 90°W, i.e., the center of the averaging box for precipitation. This anomalous convergence associated with increased precipitation (Figure 3c) is balanced by both vorticity advection (Figure 4e), with more than half contributed by $-\beta\overline{v}$, and frictional gain of anticyclonic vorticity (Figure 4f) with approximately equal contributions.

In short, Figure 4 shows that the anticyclonic vorticity gained from low-level divergence of wind associated with an intensified LLJ over the southern Great Plains is largely balanced by the loss of anticyclonic vorticity from near-surface friction, whereas the cyclonic vorticity gained from convergence associated with Gulf meridional wind anomalies is balanced by loss of vorticity by anomalous advection and friction. The contribution of vorticity advection from enhanced southerly winds over the southern Great Plains to central Gulf States precipitation is small, but the vorticity advection associated with intensified Gulf inflow is important for balancing the convergence over the central Gulf States. The friction term is dominant for balancing the gain of anticyclonic vorticity from divergence over the central Gulf States associated with the southern Great Plains southerly winds and a major term for balancing anomalous gain of cyclonic vorticity from convergence associated with the Gulf inflow anomaly.

In sum, Figures 3 and 4 show how southerly winds that either are weak over the southern Great Plains or strong over the Gulf of Mexico can increase precipitation over the central Gulf States. The correlations between these two wind indices are quite low on the interannual time scale in May, June, and July (Table 3). To determine the influence of these two wind indices together on precipitation over the central Gulf States, we construct another precipitation index (regP; Table 1) using the V_SGP and V_GF indices for June and July (JJ) average from 1979 to 2013 (individual monthly regressions are also calculated for reference in Table 3). This reconstructed regP index explains about 53% of the precipitation variance over the central Gulf States (i.e., that of the P_CGS index) during June and July, with nearly equal contribution from each wind index.

Since the V_SGP and V_GP indices are not correlated, a LLJ with a combination of weak V_SGP and strong V_GP provides a strong increase of precipitation over the central Gulf States (Figure 3). To test this hypothesis, we define the V_SGP-GF index as the difference between the V_SGP and the V_GF index, i.e., approximately the same as the meridional wind gradient averaged over the two boxes. As expected, this index is strongly negatively correlated with the P_CGS in June and July (−0.73 as shown in Table 3).

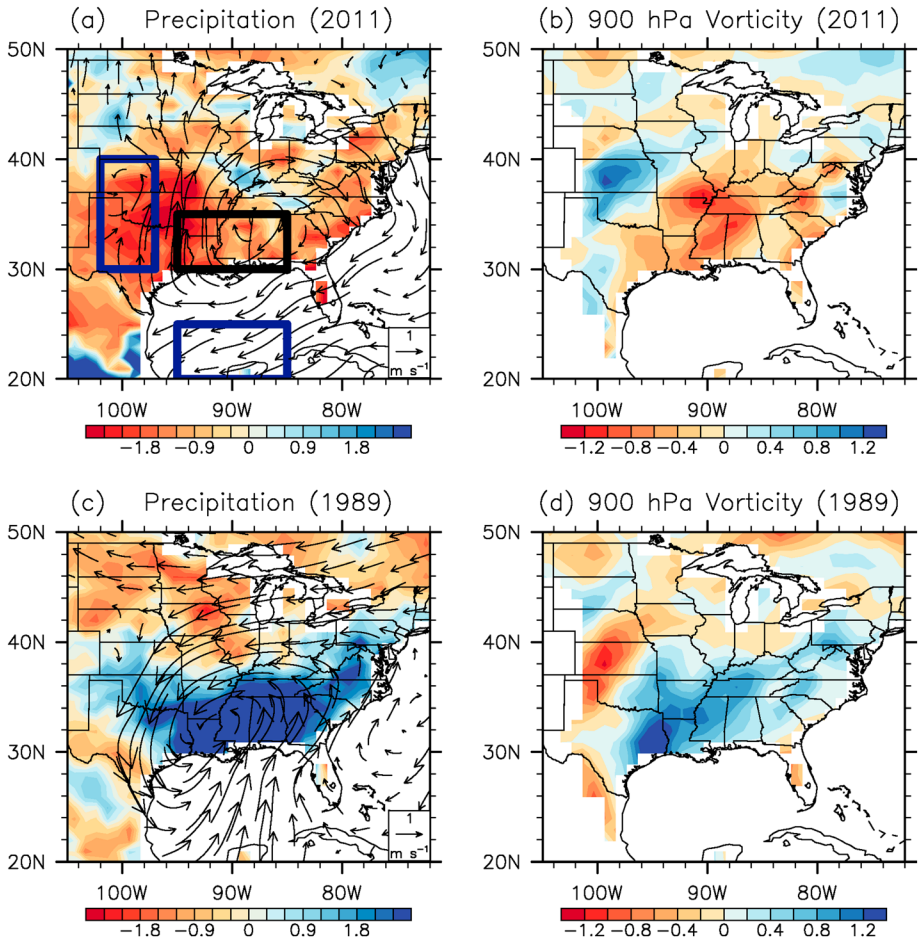

Figure 6. (a, c) Anomalies (with reference to 1979–2013 mean) of precipitation (mm d^{-1}) and 900 hPa winds (m s^{-1}), and (b, d) vorticity (10^{-5} s^{-1}) for (a, b) 2011 and (c, d) 1989. Boxes denote averaging areas for the two meridional wind indices (navy) and for the central Gulf States precipitation (black).

The year to year correspondence in June and July between the precipitation over the central Gulf States (P_CGS) and the meridional wind indices is seen in Figure 5, which shows the values of the CGS precipitation from the NARR (P_CGS; dark green and brown bars) and the reconstructed precipitation index derived from regression on the V_SGP and V_GF indices (regP; green), respectively, in order of monotonic increase of the V_SGP-GF (i.e., V_SGP-V_GF values; blue) for the period of 1979–2013. All indices are standardized, i.e., means are removed and then they are divided by their standard deviations. The observed P_CGS generally varies oppositely from the V_SGP-GF, but exceptions occur, especially for negative V_SGP-GF. In particular, the V_SGP-GF index was less than −1 standard deviation in 1985 and about −1 standard deviation in 1998, yet both had negative precipitation anomalies. Although we have not thoroughly examined precipitation for all these anomalous years, remote forcing from the tropical Pacific could be a possible explanation, e.g., 1985 was a strong La Niña year, while in 1998 La Niña developed from June to the end of the year.

Figure 6 examines June and July averaged precipitation, 900 hPa winds and vorticity anomalies for the strongest (2011) and the weakest (1989) year of the V_SGP-GF index as indicated in Figure 5. A severe drought occurred in the southern Great Plains, especially in Texas, from 2010 winter to 2011 autumn [e.g., *Seager et al*., 2014]. Precipitation over the central Gulf States also strongly decreased from its climatological mean, as indicated by the NARR, such that its June and July average in 2011 was the driest during 1979–2013 (Figure 5). Associated with this dry anomaly are enhanced southerly winds in the northern portion of the Great Plains LLJ over the southern Great Plains and reduced southerly inflow over the Gulf of Mexico (Figure 6a). Corresponding to these wind anomalies, anomalous negative vorticity is centered over the Gulf States suppressing precipitation (Figure 6b). June and July of 1989, on the other hand, is the wettest year

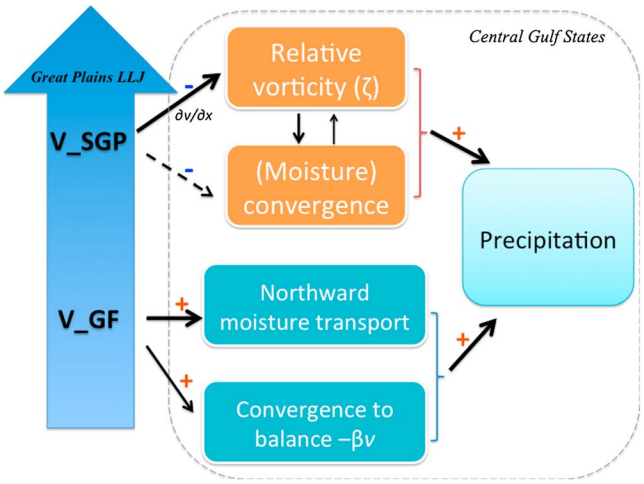

Figure 7. Schematic of the dynamical connections between the Great Plains LLJ and precipitation over the central Gulf States. "+" and "−" signs denote positive and negative relationships, respectively. The V_SGP and V_GF indices represent the meridional winds over the southern Great Plains and over the Gulf of Mexico, respectively. Black solid (dashed) line with arrowhead denotes direct (indirect) connections, and thicker lines denote stronger influences. The plot emphasizes how the LLJ affects precipitation, and the feedbacks from precipitation and vorticity/convergence changes to the jet are not explicitly shown.

for the central Gulf States from 1979 to 2013 (Figure 5). The strong positive anomaly of precipitation over the central Gulf States is associated with a weak LLJ over the southern Great Plains and an increased Gulf inflow (Figures 6c and 6d), both leading to increased moisture convergence. Figure 6 suggests that the mechanisms and connections between the LLJ and precipitation identified above are valid and useful in explaining severe dry and wet years over the central Gulf States.

In summary, interannual variability of the Great Plains LLJ, low-level vorticity, and central Gulf States precipitation are connected as follows and shown in a schematic plot in Figure 7. Increases of southerly wind over the southern Great Plains reduce vorticity on its easternside over the central Gulf States mainly through the meridional wind shear ($\partial v/\partial x$) but also the zonal wind shear ($-\partial u/\partial y$; Table 4). The reduced vorticity, in turn, leads to anomalous local divergence that suppresses precipitation. Higher correlations between the V_SGP index and 900 hPa vorticity index than that between the V_SGP and 900 hPa moisture divergence indices support this link (Table 4). This link appears to be the strongest in July as suggested by the negative correlation between the V_SGP and precipitation over the central Gulf States. The southerly Gulf inflow mainly influences the precipitation over the central Gulf States via its northward moisture transport and through its northward advection of low planetary vorticity ($-\beta v$), which requires frictional loss of cyclonic vorticity and convergence to balance.

Unlike the role of the secondary circulation at the entrance and exit areas of the subtropical jet streams in the upper troposphere [e.g., *Namias and Clapp*, 1949; *Uccellini and Kocin*, 1987], vorticity sources within the boundary layer appear to be essential for explaining the low-level convergence in our study. In the boundary layer, the frictionally caused imbalance between the geopotential height gradient and Coriolis force creates either divergence or convergence over the central Gulf States (not shown) depending on whether the winds are anomalously anticyclonic or cyclonic, as consistent with the requirement of vorticity balance.

4.2. Interaction Between Low-Level Vorticity and Convergence Over the Central Gulf States

As discussed above, a positive anomaly of the LLJ over the southern Great Plains suppresses precipitation over the central Gulf States via reducing relative vorticity and generating anomalous divergence to the east of the jet. Low-level anticyclonic vorticity is dynamically tightly coupled with divergence (or for cyclonic

Table 4. Correlations Among the Precipitation Index (P_CGS), V_SGP Index, 900 hPa Moisture Divergence (dqv900), Vorticity (vor900), and its Two Components ($-\partial u/\partial y$ and $\partial v/\partial x$) Averaged Over the Central Gulf States From 1979 to 2013[a]

Indices	JJ	May	June	July
V_SGP and vor900	**−0.73**	**−0.81**	**−0.74**	**−0.75**
V_SGP and $-\partial u/\partial y$	**−0.66**	**−0.69**	**−0.67**	**−0.57**
V_SGP and $\partial v/\partial x$	**−0.69**	**−0.77**	**−0.73**	**−0.77**
V_SGP and dqv900	**0.71**	**0.56**	**0.72**	**0.66**
P_CGS and vor900	**0.66**	*0.33*	**0.63**	**0.59**
P_CGS and dqv900	**−0.81**	**−0.69**	**−0.80**	**−0.85**
dqv900 and vor900	**−0.74**	**−0.67**	**−0.78**	**−0.67**

[a]All values are significant at the 95% confidence level (*t* test) except those in italics.

convergence). The interactions between vorticity and divergence on the hourly scale are further examined in the next sections using the NARR.

4.2.1. A Simple Vorticity Balance

A simplified vorticity balance equation can provide a rough estimate of the coupling between divergence and vorticity, i.e., how much divergence is generated by vorticity, or vice versa. In our previous study of the diurnal oscillation of the LLJ [*Pu and Dickinson*, 2014], the near surface friction was simplified to a drag term that was proportional to horizontal winds (their equations (1a) and (1b), pages 1808–1809), and the vorticity balance was written as (their equation (3), page 1815),

$$\nabla\cdot\vec{V}=-\frac{1}{f}\left(\frac{\partial\zeta}{\partial t}+\beta v+\varepsilon\zeta\right)\approx=-\frac{1}{f}(\beta v+\varepsilon\zeta), \tag{5}$$

where $\varepsilon = C_d\left|\vec{V}\right|/H$ provides a rough estimate of near surface friction due to viscosity, C_d is the surface drag term, $H = 1000$ m is the depth of the layer from surface to about 900 hPa, and $\left|\vec{V}\right|$ is the magnitude of horizontal winds averaged over the central Gulf States. As discussed earlier, the vorticity tendency is quite small; thus, a near balance is achieved among the divergence, planetary vorticity advection, and near surface friction terms, as illustrated by Figure 4. Here we assume $C_d = 0.003$ for the land surface drag coefficient, and 900 hPa monthly winds averaged over June and July are used to calculate terms in equation (5). This simple vorticity balance equation is limited in accuracy by lack of knowledge of the value of ε most appropriate to the NARR and the diurnal variability of ε.

At 32.5°N (in the middle of the central Gulf States domain), the Coriolis parameter f is about $7.836\times10^{-5}\,s^{-1}$, $\left|\vec{V}\right|$ averaged from 1979 to 2013 for June and July is about 2.6 m s^{-1}, and averaged relative vorticity ζ over the central Gulf States is about $-0.688\times10^{-5}\,s^{-1}$. Thus, the contributions from near-surface friction and from the planetary vorticity advection to divergence are $6.87\times10^{-7}\,s^{-1}$ and $-5.10\times10^{-7}\,s^{-1}$, respectively. Such an estimate is quite rough, as the frictional term is expected to have substantial error, and their sum, as a difference between two large numbers, is expected to be even more inaccurate. However, the magnitude of the divergence estimated from equation (5) is not very different from (i.e., 30% less than) the divergence averaged over the central Gulf States based on the NARR. In addition, the correlation between the June and July averaged divergence derived from vorticity advection and friction terms determined above and the divergence over the central Gulf States from the NARR is 0.62 during 1979–2013, i.e., explains about 38% of the total variance of the divergence for the period of 1979–2013. Given the simple assumptions made to estimate surface friction, these results are not inconsistent with a significant or dominant contribution of vorticity to low-level divergence in the atmospheric boundary layer.

4.2.2. Dynamic Links Between the LLJ, Vorticity, Divergence, and Precipitation Over the Central Gulf States Inferred from Empirical Relationships on the Hourly Scale

Does variability of the southerly flow over the southern Great Plains influence that of the low-level vorticity field, or is it a result of the low-level vorticity variation? Our analysis focuses on the influence of the LLJ on vorticity and divergence over the central Gulf States, but conversely variability of the large-scale vorticity field could affect the LLJ. A full understanding of this question may require model simulations; here we show empirical evidence from the 3 h resolution reanalysis that the jet can lead to changes of local vorticity when the southerly wind over the southern Great Plains is strong. Figure 8 shows the 3-hourly lead-lag correlations among the indices of precipitation over the central Gulf States (P_CGS), V_SGP, and 900 hPa vorticity and convergence over the central Gulf States in July. Values are selected when the 3-hourly V_SGP index is equal to or greater than its two standard deviations in July (i.e., time 0) and those from one day before (Lead 8) to one day after (Lag 8). "Lag n" on the x axis denotes that one variable lags the other by $3\times n$ hours, likewise for "Lead n." Taking the red line as an example, its largest value at "Lag 5" marked by the symbol "star" shows the correlation coefficient for convergence lagging vorticity by 15 h is the greatest compared to all other lead and lag correlation coefficients shown in Figure 8. The two standard deviations criterion is used to select extremely strong events. Contemporary correlation between the jet and vorticity would be the strongest of all lead and lag correlations, if we had to used one standard deviation to include more frequently occurred LLJ variations.

The highest correlations (stars) show that changes of the V_SGP lead the vorticity by 3 h (blue), while changes of vorticity lead convergence by 15 h (red). Note that the coupling between convergence and vorticity is quite tight, and there is a slightly weaker peak of the correlation when convergence leads vorticity by about 12 h. Change of precipitation also lags vorticity by 3 h (yellow), suggesting that a decrease of vorticity can lead

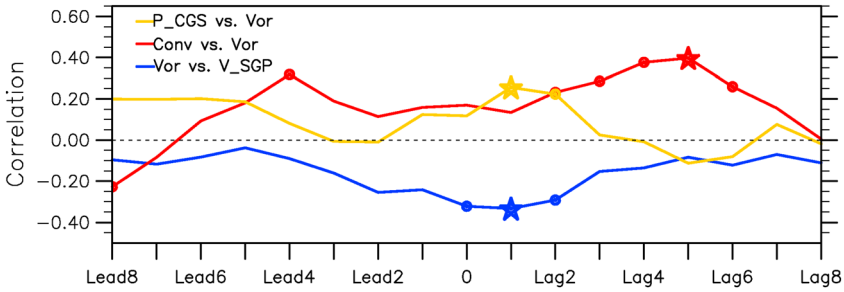

Figure 8. The 3-hourly lead-lag Spearman rank order correlations between indices of CGS precipitation (P_CGS) and 900 hPa vorticity (Vor; yellow), CGS 900 hPa convergence (Conv) and vorticity (red), and CGS 900 hPa vorticity and V_SGP (blue) in July when the V_SGP index is equal or greater than its two standard deviations (see details in section 4.2.2). *x* axis shows 3-hourly lead or lag intervals. Correlation coefficients significant at the 95% confidence levels (*t* test) are marked by filled circles, and the largest coefficients (in absolute value) are denoted by stars.

to precipitation reduction. The above lead-lag correlations appear to support the link of enhanced southerly wind resulting in reduced vorticity and then enhanced divergence, although the second peak of the correlation between convergence and vorticity at Lead 4 implies some influence of convergence on vorticity as well. Likewise, decreases of precipitation can also lead to divergence and negative vorticity, which may be inferred from the longer response time of convergence to vorticity (peak at 15 h) than the time lag (peak at 3 h) of precipitation in response to vorticity. Such a feedback is broadly consistent with our hypothesis that low-level wind variability leads to changes of vorticity. Also note both convergence and precipitation have significant lag correlations with vorticity at 6 h (Lag 2), indicating a nearly instantaneous coupling between convergence and precipitation as well.

5. Conclusions

This paper examines the connection among the Great Plains low-level jet (LLJ), low-level vorticity, and precipitation on the eastern side of the jet over the central Gulf States on the interannual time scale. It is found that variations of central Gulf States precipitation during June and July are strongly controlled by winds represented by two nearly uncorrelated wind indices that represent the variability of meridional winds at the southern Great Plains (30°–40°N) and its southerly inflow over the Gulf of Mexico.

Our analysis suggests that the meridional wind over the southern Great Plains has a strong control on relative vorticity over the central Gulf States region via its influence on both the zonal and meridional wind shears ($-\partial u/\partial y$ and $\partial v/\partial x$, Table 4), with stronger southerly winds generating anomalous negative vorticity to its east, leading to local moisture divergence and consequently reducing precipitation. The meridional winds over the southern Great Plains appear to have a stronger control on vorticity over the central Gulf States than on moisture convergence. The negative correlation between the Great Plains LLJ and precipitation over the central Gulf States therefore may be decomposed into a chain of effects involving the influence of LLJ on vorticity, coupling between vorticity, moisture divergence, and precipitation over the central Gulf States. On the other hand, the southerly Gulf inflow is positively correlated with central Gulf States precipitation and its influence on precipitation is largely associated with its anomalous northward moisture transport and dynamical balances that promote local moisture convergence in the central Gulf States.

Our vorticity budget analysis suggests that the anticyclonic vorticity generated by anomalous divergence associated with strong southerly flow over the southern Great Plains is mainly balanced by its frictional loss, whereas for strong Gulf inflow, the cyclonic vorticity generated from convergence over the central Gulf States is largely balanced by losses from friction and by enhanced negative northward advection of planetary vorticity.

Together these two uncorrelated LLJ indices can explain about 53% of the precipitation variance over the central Gulf States in June and July on the interannual time scale. The most effective configuration for the LLJ to decrease precipitation over the central Gulf States is when the difference between LLJ over the southern Great Plains and that over Gulf of Mexico is the greatest, i.e., when there is a strong positive difference due to a strong southerly wind over the southern Great Plains and a weak southerly inflow over the Gulf of Mexico (e.g., in 2011). Likewise, the strongest negative such difference appears to be most effective for increasing precipitation over the central Gulf States (e.g., in 1989).

Acknowledgments
We thank the three anonymous reviewers for their extremely thorough and constructive comments that lead to substantial improvement of this work. The North American Regional Reanalysis used in this paper is available to download from http://www.esrl.noaa.gov/psd/data/gridded/data.narr.html. This work was supported by a grant from the U.S. Department of Energy DOE (DE-FG02-09ER64746), the NASA Indicators for the National Climate Assessment Program (grant NNX13AN39G), and NOAA's Climate Program Office's Modeling, Analysis, Predictions, and Projections Program (grant award NA10OAR4310157).

References

Arritt, R. W., and M. J. Mitchell (1994), Variability of the Great Plains low-level jet and its influence on mesoscale convection, in *Proceedings Sixth Conference on Mesoscale Processes*, pp. 151–153, Amer. Meteorol. Soc, Portland, OR.

Helfand, H. M., and S. D. Schubert (1995), Climatology of the simulated Great Plains low-level Jet and its contribution to the continental moisture budget of the United-States, *J. Clim.*, *8*(4), 784–806, doi:10.1175/1520-0442(1995)008<0784:Cotsgp>2.0.Co;2.

Hering, W. S., and T. R. Borden (1962), Diurnal variations in the summer wind field over the central United States, *J. Atmos. Sci.*, *19*(1), 81–86, doi:10.1175/1520-0469(1962)019<0081:Dvitsw>2.0.Co;2.

Higgins, R. W., Y. Yao, E. S. Yarosh, J. E. Janowiak, and K. C. Mo (1997), Influence of the Great Plains low-level jet on summertime precipitation and moisture transport over the central United States, *J. Clim.*, *10*(3), 481–507, doi:10.1175/1520-0442(1997)010<0481:Iotgpl>2.0.Co;2.

Li, L. F., W. H. Li, and Y. Kushnir (2012), Variation of the North Atlantic subtropical high western ridge and its implication to Southeastern US summer precipitation, *Clim. Dyn.*, *39*(6), 1401–1412, doi:10.1007/s00382-011-1214-y.

Li, W. H., L. F. Li, R. Fu, Y. Deng, and H. Wang (2011), Changes to the North Atlantic subtropical high and its role in the intensification of summer rainfall variability in the southeastern United States, *J. Clim.*, *24*(5), 1499–1506, doi:10.1175/2010jcli3829.1.

Mesinger, F., et al. (2006), North American regional reanalysis, *Bull. Am. Meteorol. Soc.*, *87*(3), 343–360, doi:10.1175/Bams-87-3-343.

Mo, K. C., and J. E. Schemm (2008), Relationships between ENSO and drought over the southeastern United States, *Geophys. Res. Lett.*, *35*, L15701, doi:10.1029/2008GL034656.

Mo, K. C., J. N. Paegle, and R. W. Higgins (1997), Atmospheric processes associated with summer floods and droughts in the central United States, *J. Clim.*, *10*(12), 3028–3046, doi:10.1175/1520-0442(1997)010<3028:Apawsf>2.0.Co;2.

Namias, J., and P. F. Clapp (1949), Confluence theory of the high tropospheric jet stream, *J. Meteorol.*, *6*(5), 330–336, doi:10.1175/1520-0469(1949)006<0330:CTOTHT>2.0.CO;2.

North, G. R., T. L. Bell, R. F. Cahalan, and F. J. Moeng (1982), Sampling errors in the estimation of empirical orthogonal functions, *Mon. Weather Rev.*, *110*, 699–706, doi:10.1175/1520-0493(1982)110<0699:SEITEO>2.0.CO;2.

Pitchford, K. L., and L. London (1962), The low-level jet as related to nocturnal thunderstorms over Midwest United States, *J. Appl. Meteorol.*, *1*, 43–47, doi:10.1175/1520-0450(1962)001<0043:TLLJAR>2.0.CO;2.

Pu, B., and R. E. Dickinson (2014), Diurnal spatial variability of Great Plains summer precipitation related to the dynamics of the low-level jet, *J. Atmos. Sci.*, *71*(5), 1807–1817, doi:10.1175/Jas-D-13-0243.1.

Rasmusson, E. M. (1967), Atmospheric water vapor transport and water balance of North America. I. Characteristics of water vapor flux field, *Mon. Weather Rev.*, *95*(7), 403, doi:10.1175/1520-0493(1967)095<0403:Awvtat>2.3.Co;2.

Ruane, A. C. (2010), NARR's atmospheric water cycle components. Part I: 20-year mean and annual interactions, *J. Hydrometeorol.*, *11*(6), 1205–1219, doi:10.1175/2010jhm1193.1.

Ruiz-Barradas, A., and S. Nigam (2006), Great plains hydroclimate variability: The view from North American regional reanalysis, *J. Clim.*, *19*(12), 3004–3010, doi:10.1175/Jcli3768.1.

Schubert, S. D., H. M. Helfand, C. Y. Wu, and W. Min (1998), Subseasonal variations in warm-season moisture transport and precipitation over the central and eastern United States, *J. Clim.*, *11*(10), 2530–2555, doi:10.1175/1520-0442(1998)011<2530:Sviwsm>2.0.Co;2.

Seager, R., A. Tzanova, and J. Nakamura (2009), Drought in the southeastern United States: Causes, variability over the last millennium, and the potential for future hydroclimate change, *J. Clim.*, *22*(19), 5021–5045, doi:10.1175/2009jcli2683.1.

Seager, R., L. Goddard, J. Nakamura, N. Henderson, and D. E. Lee (2014), Dynamical causes of the 2010/11 Texas-Northern Mexico drought*, *J. Hydrometeorol.*, *15*(1), 39–68, doi:10.1175/Jhm-D-13-024.1.

Uccellini, L. W., and P. J. Kocin (1987), The interaction of jet streak circulations during heavy snow events along the east coast of the United States, *Weather Forecast.*, *2*, 289–308, doi:10.1175/1520-0434(1987)002<0289:TIOJSC>2.0.CO;2.

Wang, H., R. Fu, A. Kumar, and W. H. Li (2010), Intensification of summer rainfall variability in the southeastern United States during recent decades, *J. Hydrometeorol.*, *11*(4), 1007–1018, doi:10.1175/2010jhm1229.1.

Weaver, S. J., and S. Nigam (2008), Variability of the great plains low-level jet: Large-scale circulation context and hydroclimate impacts, *J. Clim.*, *21*(7), 1532–1551, doi:10.1175/2007jcli1586.1.

Weaver, S. J., and S. Nigam (2011), Recurrent supersynoptic evolution of the Great Plains low-level jet, *J. Clim.*, *24*(2), 575–582, doi:10.1175/2010jcli3445.1.

Weaver, S. J., A. Ruiz-Barradas, and S. Nigam (2009), Pentad evolution of the 1988 drought and 1993 flood over the Great Plains: An NARR perspective on the atmospheric and terrestrial water balance, *J. Clim.*, *22*(20), 5366–5384, doi:10.1175/2009jcli2684.1.

Zhu, J. H., and X. Z. Liang (2013), Impacts of the Bermuda high on regional climate and ozone over the United States, *J. Clim.*, *26*(3), 1018–1032, doi:10.1175/Jcli-D-12-00168.1.